




# AIM2 upregulation promotes metastatic progression and PD-L1 expression in lung adenocarcinoma

Jing-Quan Zheng<sup>1,2,3</sup> | Che-Hsuan Lin<sup>4,5</sup> | Hsun-Hua Lee<sup>6,7,8</sup> | Wei-Ming Chang<sup>9</sup>  | Li-Jie Li<sup>10</sup> | Chia-Yi Su<sup>11</sup> | Kang-Yun Lee<sup>1,2,3</sup> | Hui-Wen Chiu<sup>1,12,13</sup>  | Yuan-Feng Lin<sup>1,14</sup> 

<sup>1</sup>Graduate Institute of Clinical Medicine, College of Medicine, Taipei Medical University, Taipei, Taiwan

<sup>2</sup>Division of Pulmonary Medicine, Department of Internal Medicine, Shuang Ho Hospital, Taipei Medical University, New Taipei City, Taiwan

<sup>3</sup>Division of Pulmonary Medicine, Department of Internal Medicine, School of Medicine, College of Medicine, Taipei Medical University, Taipei, Taiwan

<sup>4</sup>Department of Otolaryngology, Taipei Medical University Hospital, Taipei Medical University, Taipei, Taiwan

<sup>5</sup>Department of Otolaryngology, School of Medicine, College of Medicine, Taipei Medical University, Taipei, Taiwan

<sup>6</sup>Department of Neurology, Taipei Medical University Hospital, Taipei Medical University, Taipei, Taiwan

<sup>7</sup>Department of Neurology, School of Medicine, College of Medicine, Taipei Medical University, Taipei, Taiwan

<sup>8</sup>Dizziness and Balance Disorder Center, Shuang Ho Hospital, Taipei Medical University, New Taipei City, Taiwan

<sup>9</sup>School of Oral Hygiene, College of Oral Medicine, Taipei Medical University, Taipei, Taiwan

<sup>10</sup>Ph.D. Program of School of Dentistry, College of Oral Medicine, Taipei Medical University, Taipei, Taiwan

<sup>11</sup>Department of Pharmacology, University of Minnesota Medical School, Minneapolis, Minnesota, USA

<sup>12</sup>Department of Medical Research, Shuang Ho Hospital, Taipei Medical University, New Taipei City, Taiwan

<sup>13</sup>TMU Research Center of Urology and Kidney, Taipei Medical University, Taipei, Taiwan

<sup>14</sup>Cell Physiology and Molecular Image Research Center, Wan Fang Hospital, Taipei Medical University, Taipei, Taiwan

## Correspondence

Hui-Wen Chiu and Yuan-Feng Lin,  
Graduate Institute of Clinical Medicine,  
College of Medicine, Taipei Medical  
University, 250 Wu-Hsing Street, Taipei  
11031, Taiwan.

Emails: [leu3@tmu.edu.tw](mailto:leu3@tmu.edu.tw);  
[d001089012@tmu.edu.tw](mailto:d001089012@tmu.edu.tw)

## Funding information

Ministry of Science and Technology,  
Taiwan, Grant/Award Number: MOST  
108-2314-B-038-016 and MOST  
108-2320-B-038-017-MY3

## Abstract

Cancer metastasis leading to the dysfunction of invaded organs is the main cause of the reduced survival rates in lung cancer patients. However, the molecular mechanism for lung cancer metastasis remains unclear. Recently, the increased activity of inflammasome appeared to correlate with the metastatic progression and immunosuppressive ability of various cancer types. Our results showed that the mRNA levels of absence in melanoma 2 (AIM2), one of the inflammasome members, are extensively upregulated in primary tumors compared with normal tissues derived from the TCGA lung adenocarcinoma (LUAD) database. Moreover, Kaplan-Meier analysis demonstrated that a higher mRNA level of AIM2 refers to a poor prognosis in LUAD patients. Particularly, AIM2 upregulation is closely correlated with smoking history and the absence of *EGFR/KRAS/ALK* mutations in LUAD. We further showed that the endogenous mRNA levels of AIM2 are causally associated with the metastatic potentials of the tested LUAD cell lines. AIM2 knockdown suppressed but overexpression promoted the migration ability and lung colony-forming ability of tested LUAD cells.

**Abbreviations:** AIM2, absence in melanoma 2; CARD, caspase activation and recruitment domain; EMT, epithelial-mesenchymal transition; GBPs, guanylate-binding proteins; GEO, Gene Expression Omnibus; IFN- $\gamma$ , interferon gamma; IL-1 $\beta$ , interleukin 1 $\beta$ ; LUAD, lung adenocarcinoma; LUSC, lung squamous cell carcinoma; NLR, nucleotide-binding leucine-rich repeat-containing receptor; NSCLC, non-small cell lung cancer; PD-L1, programmed cell death-ligand 1; SCLC, small cell lung cancer; TCGA, The Cancer Genome Atlas.

This is an open access article under the terms of the [Creative Commons Attribution-NonCommercial-NoDerivs](https://creativecommons.org/licenses/by-nc-nd/4.0/) License, which permits use and distribution in any medium, provided the original work is properly cited, the use is non-commercial and no modifications or adaptations are made.

© 2022 The Authors. *Cancer Science* published by John Wiley & Sons Australia, Ltd on behalf of Japanese Cancer Association.

In addition, we found that AIM2 upregulation is closely associated with an increased level of immune checkpoint gene set, as well as programmed cell death-ligand 1 (PD-L1) transcript, in TCGA LUAD samples. AIM2 knockdown predominantly repressed but overexpression enhanced PD-L1 expression via altering the activity of PD-L1 transcriptional regulators NF- $\kappa$ B/STAT1 in LUAD cells. Our results not only provide a possible mechanism underlying the AIM2-promoted metastatic progression and immune evasion of LUAD but also offer a new strategy for combating metastatic/immunosuppressive LUAD via targeting AIM2 activity.

#### KEYWORDS

AIM2 inflammasome, cancer metastasis, epithelial-mesenchymal transition, lung cancer, PD-L1

## 1 | INTRODUCTION

Lung cancer is mainly classified into non-small cell lung cancer (NSCLC) with approximately 15% for the 5-year survival rate of patients<sup>1</sup> and small cell lung cancer (SCLC) with about 6% for the 5-year survival rate of patients.<sup>2</sup> NSCLC is further classified into three subtypes: adenocarcinoma, squamous-cell carcinoma, and large-cell carcinoma. The metastatic progression is known as a leading cause for the death of lung cancer patients. Lung carcinoma has been found to preferentially metastasize to bone (34.3%), lung (32.1%), brain (28.4%), adrenals (16.7%), and liver (13.4%).<sup>3</sup> Besides, the inflammatory condition of tumor microenvironment has been considered a critical factor to determine the therapeutic sensitivity and clinical outcome of lung cancer patients.<sup>4</sup> Tumor-infiltrating immune cells and chronic inflammation have been also thought to be important factors for cancer development and prognosis in NSCLC patients.<sup>5</sup> However, the involvement of inflammation-related pathways in triggering the metastatic progression and immunosuppression in NSCLC is still unclear.

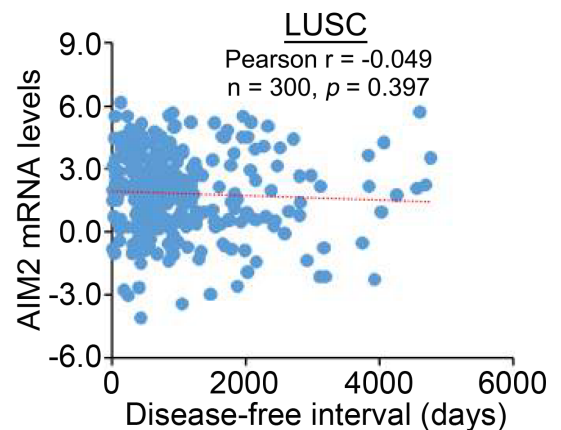
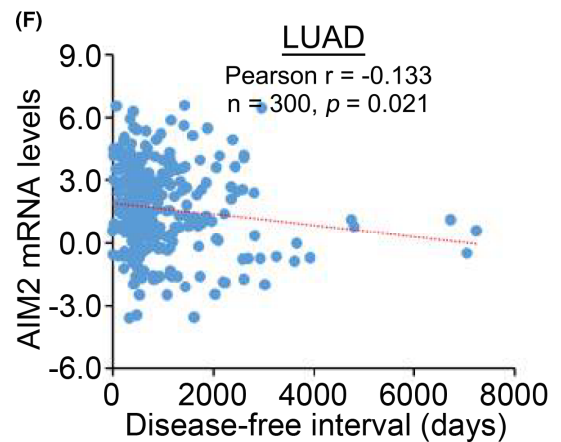
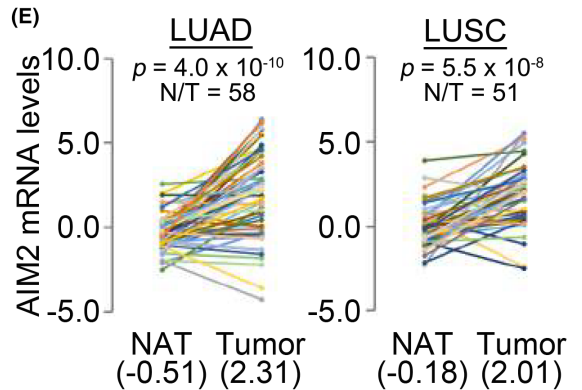
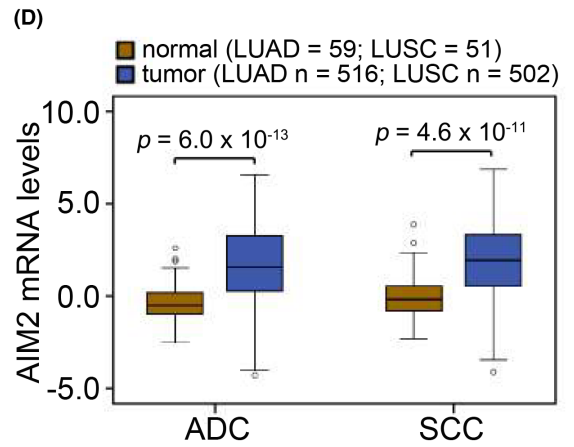
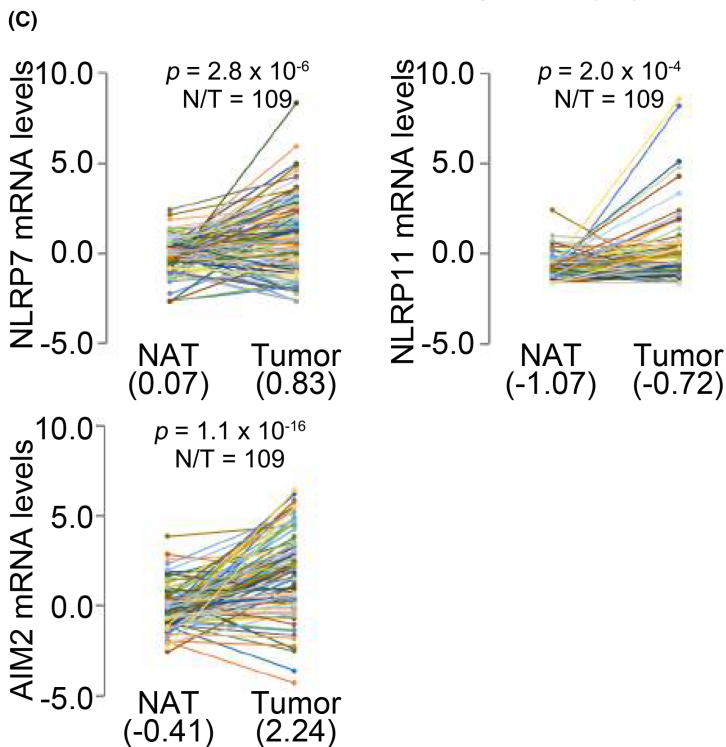
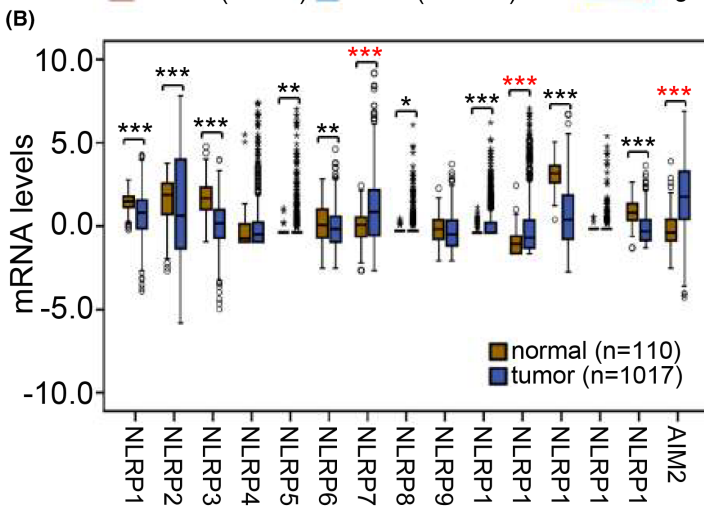
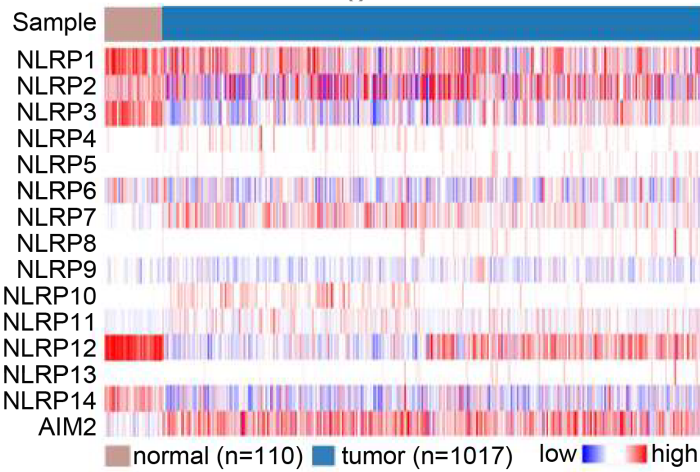
Inflammasomes are primarily identified in myeloid cells and known as intracellular multiprotein signaling complexes.<sup>6</sup> They generally consist of an innate immune receptor either from the nucleotide-binding leucine-rich repeat-containing receptor (NLR) family or absent in melanoma 2 (AIM2). They assemble around a cytoplasmic receptor of the NLR family even though other cytoplasmic receptors like pyrin are also able to form inflammasomes. In general, upon detection of a microbial, a danger or a homeostasis pattern by the receptor, the nucleation of the multiprotein-scaffolding platform occurs. Sequentially, inflammasome receptors utilize their caspase activation and recruitment domain (CARD) to interact with

the adaptor protein apoptosis-associated speck-like protein containing a CARD (ASC) through homotypic domain interactions, which then recruits and activates procaspase-1 via proteolytic cleavage and ultimately promotes the secretion of proinflammatory IL1 $\beta$  and IL18 cytokines and pyroptosis.<sup>7</sup> Recent reports have demonstrated the role of inflammasome in modulating tumorigenesis and cancer progression, for example, drug resistance and cancer metastasis. Whereas the NLRP3 inflammasome functions as a negative regulator of tumorigenesis during colitis-associated cancer,<sup>8</sup> the activation of NLRP3 inflammasome plays a pivotal role in the tumor growth of breast cancer.<sup>9</sup> Moreover, the activation of inflammasome has been shown to be involved in the mechanism for radiotherapy resistance in breast cancer.<sup>10</sup> Several lines of evidence also revealed that the activity of inflammasome is required for the metastatic progression in breast,<sup>11</sup> head and neck,<sup>12</sup> colon<sup>13</sup> and gastric<sup>14</sup> cancers. In lung cancer, the activity of NLRP3 inflammasome appeared to modulate the proliferation and metastasis of NSCLC cells.<sup>15,16</sup> Nevertheless, the mechanism by which inflammasome fosters the metastatic progression of lung cancer remains largely unknown.

This study aimed to investigate the prognostic significance and oncogenic function of inflammasome in lung cancer. We found that AIM2 expression is predominantly upregulated in primary tumors compared with normal tissues derived from patients with lung cancer. Moreover, AIM2 expression was negatively correlated with disease-free interval in lung adenocarcinoma (LUAD), not lung squamous cell carcinoma (LUSC), patients and positively correlated with the metastatic/immunosuppressive capacity of LUAD cells. Our results provide a new therapeutic strategy to combat metastatic/immunosuppressive LUAD via targeting the AIM2-related signaling axis.

**FIGURE 1** AIM2 is highly expressed in primary tumors compared with normal tissues and correlates with a shorter disease-free interval in lung adenocarcinoma (LUAD). Heatmap (A) and boxplot (B) for the transcriptional profiling of inflammasome family in normal lung tissues and primary tumors from TCGA lung cancer database. C, The mRNA levels of *NLRP7*, *NLRP11*, and *AIM2* in the paired normal adjacent tissue and primary tumor derived from clinical lung cancer patients in TCGA database. D, Boxplot for the mRNA levels of AIM2 in the normal tissues and primary tumors from patients with LUAD or lung squamous cell carcinoma (LUSC). *P*-values (B, D), Student *t* test. E, The mRNA levels of AIM2 in the paired normal adjacent tissue and primary tumor derived from patients with LUAD and LUSC. *P*-values (C, E), paired *t* test. F, Scatter plots for the mRNA levels of AIM2 and disease-free intervals in TCGA LUAD and LUSC. *p*-value, Pearson correlation test. The symbols \*, \*\* and \*\*\* denote  $p < 0.01$ ,  $p < 0.05$  and  $p < 0.001$ , respectively.

## (A) TCGA Lung Cancer Database



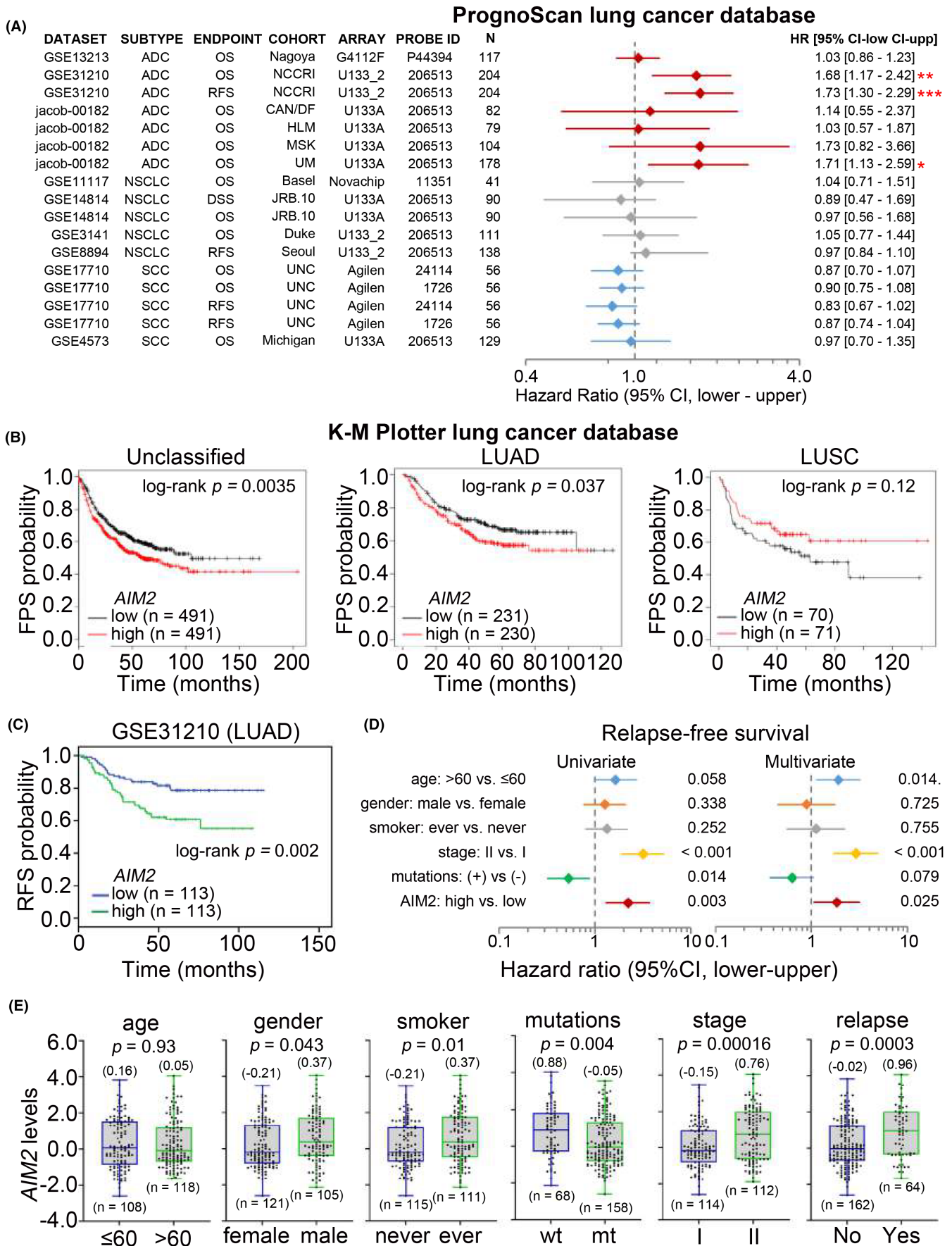


FIGURE 2 Legend on next page

**FIGURE 2** AIM2 upregulation correlates with poor outcomes in lung adenocarcinoma (LUAD). A, Cox regression test using univariate model for AIM2 mRNA levels (high vs. low) against different lung cancer datasets deposited in Prognoscan database. \* $p < 0.01$ , \*\* $p < 0.05$ , \*\*\* $p < 0.001$ . Kaplan-Meier analyses for AIM2 transcripts under the condition of first progression-free survival (FPS) (B) and recurrence-free survival (RFS) (C) probability in the unclassified lung cancer patients and the patients with LUAD and lung squamous cell carcinoma (LUSC) from K-M Plotter database and with LUAD from the GSE31210 dataset, respectively. D, Cox regression test using univariate and multivariate models against age, gender, smoker, stage, EGFR/ALK/KRAS mutations, and AIM2 mRNA levels under the condition of RFS probability in GSE31210 LUAD patients. E, Boxplots for the AIM mRNA levels in the indicated stratifications. The inserts represent the median of AIM2 mRNA levels and number of patients. The statistical significances were analyzed by  $t$  test.

## 2 | MATERIALS AND METHODS

### 2.1 | Data collection and processing from online genomic databases

The transcriptional profiles of the NLRP family and AIM2 in normal tissues and primary tumors and clinicopathological results derived from The Cancer Genome Atlas (TCGA) lung cancer patients were downloaded from the UCSC Xena website (<http://xena.ucsc.edu/welcome-to-ucsc-xena/>). The information of a meta-analysis against the AIM2 transcript was obtained from Prognoscan website (<http://dna00.bio.kyutech.ac.jp/Prognoscan/index.html>). Kaplan-Meier analyses for AIM2 mRNA levels using overall and first progression-free survival probability were performed by using the lung cancer database on the Kaplan-Meier Plotter website (<http://kmpplot.com/analysis/>). Microarray results and clinical information of the Gene Expression Omnibus (GEO) dataset GSE31210 were downloaded from the GEO website.

### 2.2 | Cell lines and cell culture condition

Lung adenocarcinoma cell lines A549, H1355, HCC827, and PC9 were obtained from the American Type Culture Collection (ATCC) and maintained in RPMI1640 media supplemented with 10% fetal bovine serum (FBS). 293T cells were also obtained from ATCC, cultivated in Dulbecco's modified Eagle's medium (DMEM) containing 10% FBS, and incubated at 37°C with 5% CO<sub>2</sub>. All cell culture media and supplements were purchased from Gibco BRL.

### 2.3 | Cell migration assay

Cellular migration ability was detected by the transwell cultivation for 16 hours using the Boyden Chamber Assay (NeuroProbe) as shown in our previous report.<sup>17</sup> For neutralization of IL-1 $\beta$  and IL18, A549 cells ( $1.5 \times 10^4$ ) were pretreated without or with rabbit anti-IL-1 $\beta$  (#41059; SAB) and IL18/nonimmunized control (#10119-T52/#CR1; Sino Biological) polyclonal antibodies at 10  $\mu$ g/ml for 24 hours prior to performing cellular migration assay. The migrated cells were observed under a microscope (Olympus) at 400 $\times$  magnification and quantified by counting the cells in three random areas.

### 2.4 | Statistical analysis

IBM SPSS Statistics 19.0 software (IBM) was used to analyze statistical significance.  $t$  test and paired  $t$  test were used to estimate the statistical significance of AIM mRNA levels in TCGA and GSE31210 samples. Pearson and Spearman correlation tests were used to analyze the statistical significance of parametric and nonparametric data, respectively. Kaplan-Meier analysis and the log-rank test were used to evaluate the survival probabilities under the designated survival conditions. Nonparametric two independent samples and three or more related samples were analyzed by the Mann-Whitney  $U$  test and Friedman test, respectively. In all statistical analyses,  $P$ -values lower than 0.05 were considered to be statistically significant.

Additional materials and methods are available in [Supporting Information](#).

## 3 | RESULTS

### 3.1 | AIM2 upregulation is extensively found in primary tumors and negatively correlates with disease-free interval in LUAD

We first determined the transcriptional profiling of the NLR family and AIM2 in TCGA lung cancer patients (Figure 1A) and found that *NLRP7*, *NLRP11*, and *AIM2* mRNA levels are upregulated but *NLRP1*, *NLRP2*, *NLRP3*, *NLRP5*, *NLRP6*, *NLRP8*, *NLRP10*, *NLRP12*, and *NLRP14* mRNA levels are downregulated significantly ( $p < 0.0001$ ) in primary tumors compared with normal tissues (Figure 1B). We further examined the transcriptional levels of *NLRP7*, *NLRP11*, and *AIM2* in the paired normal adjacent tissues and primary tumors derived from TCGA lung cancer patients. In comparison with *NLRP7* and *NLRP11*, the increased levels of the *AIM2* transcript in primary tumors compared with normal adjacent tissues were more predominant (Figure 1C). Moreover, *AIM2* expression in LUAD and LUSC was significantly higher than that of the respective normal tissues derived from TCGA lung cancer patients (Figure 1D). Similar findings were noted in the paired normal adjacent tissues and primary tumors from LUAD and LUSC (Figure 1E). In addition, immunohistochemistry data revealed that the protein levels of AIM2 in LUAD are potentially higher than those of alveolar cells from normal lung tissues (Figure S1A,B). We also found a statistically ( $p = 0.021$ ) negative correlation between *AIM2*, not *NLRP7* and *NLRP11* (Figure S2), mRNA

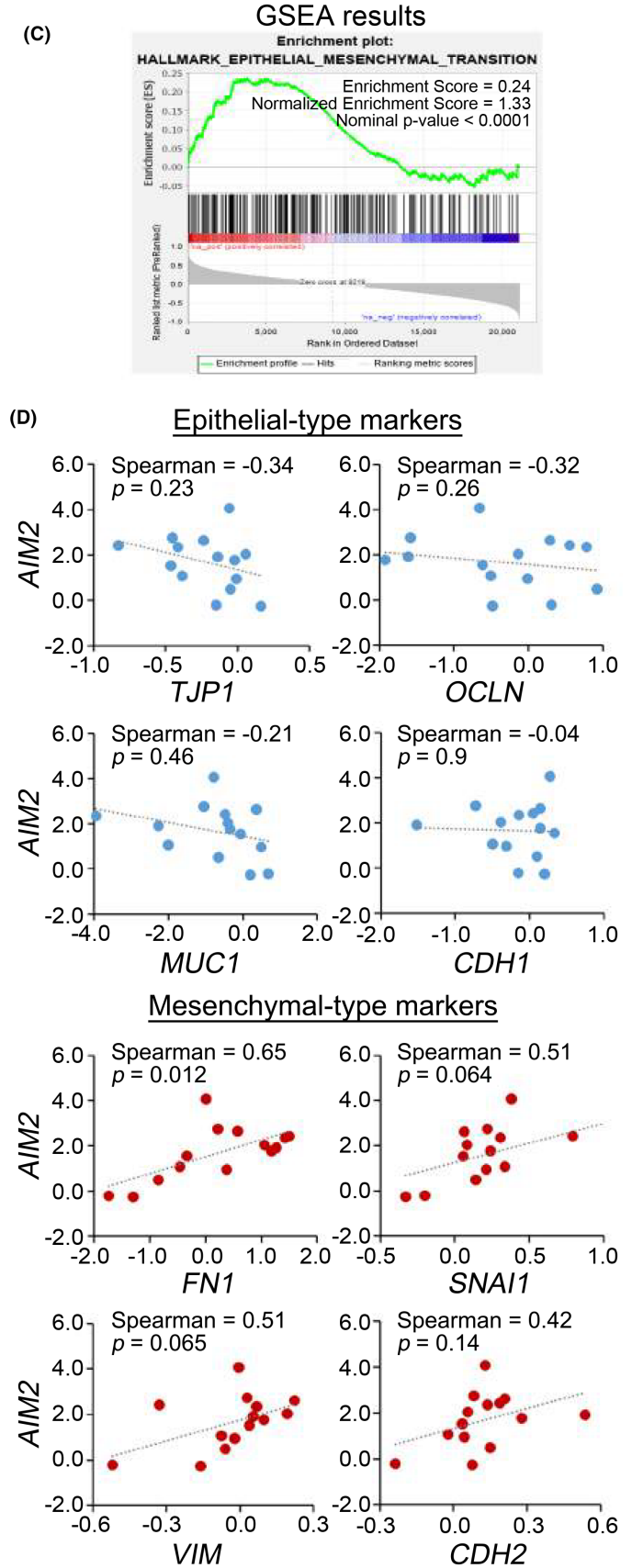
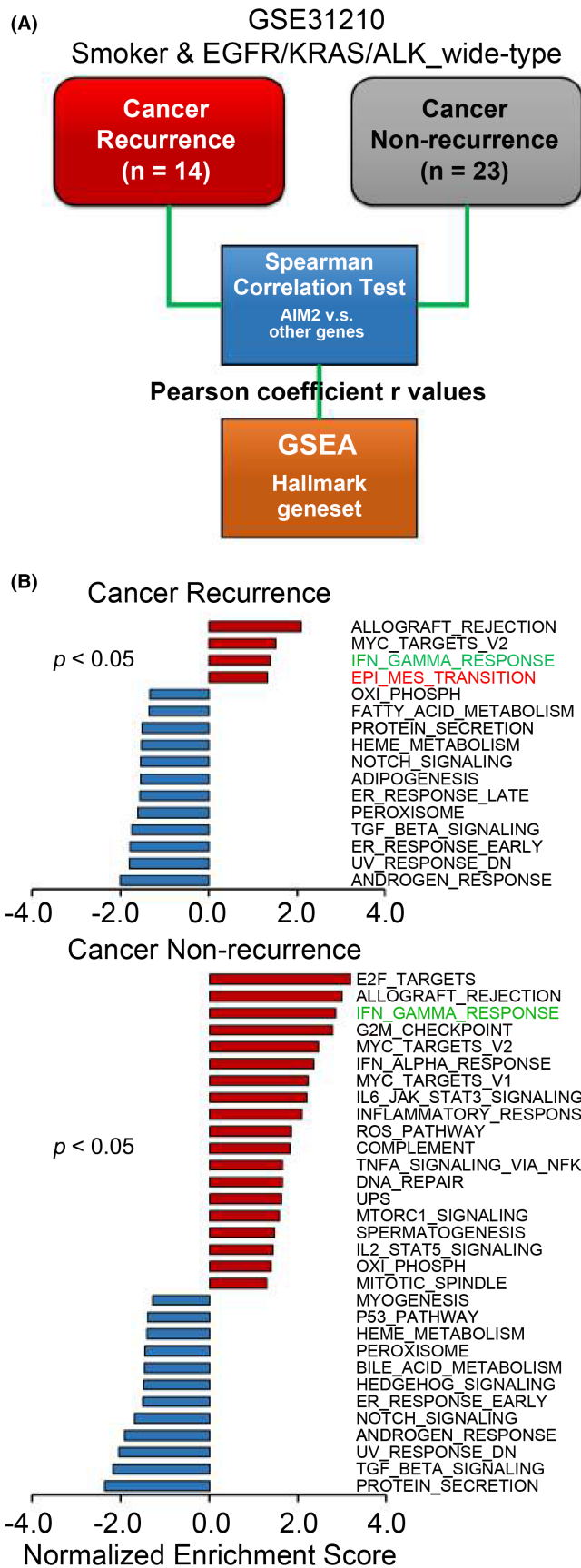


FIGURE 3 Legend on next page

**FIGURE 3** AIM2 upregulation correlates with the activation of epithelial-mesenchymal transition (EMT) in the primary tumors derived from lung adenocarcinoma (LUAD) patients with cancer recurrence. A, The flowchart for generating the AIM2-related gene signature from the primary tumors of GSE31210 LUAD patients and performing the computational simulation using the Gene Set Enrichment Analysis (GSEA) program against the Hallmark gene set. B, Histogram for the normalized enrichment scores derived from GSEA simulation against the correlation between AIM2-related gene signature and Hallmark gene set. C, The plot of enrichment score was obtained from the correlation between the AIM2-related gene signature and EMT-related gene set in the GSEA simulation. D, Scatchard plots for the mRNA levels of AIM2- and EMT-related genes *TJP1*, *OCLN*, *MUC1*, *CDH1*, *FN1*, *SNAI1*, *VIM*, and *CDH2* in the primary tumors of GSE31210 LUAD patients with cancer recurrence as shown in (A). *p*-values, Spearman correlation test.

levels and the disease-free interval of patients in TCGA LUAD, but not LUSC (Figure 1F).

### 3.2 | AIM2 upregulation predicts a poor prognosis and serves as an independent prognostic marker in LUAD

The data obtained from Prognoscan demonstrated that a higher AIM2 level potentially correlates with an increased hazard ratio in the cohorts with LUAD but may predict a favorable outcome in the cohorts with LUSC (Figure 2A). Moreover, Kaplan-Meier analyses derived from the K-M Plotter lung cancer database revealed that a higher AIM2 transcript determined by the median of its mRNA levels in the tumors of the enrolled lung cancer patients potentially correlates with a poorer overall (Figure S3A) and first progression-free (Figure 2B) survival probability in patients with unclassified lung cancer and LUAD, but not LUSC.

Under the condition of overall (Figure S3B) and recurrence-free survival (Figure 3C) probabilities, the high-level AIM2 transcript was associated with poor prognosis in GSE31210 LUAD patients. Cox regression test using univariate and multivariate modes revealed that AIM2 expression (high vs. low) acts as an independent prognostic factor under recurrence-free (Figure 2D), not overall (Figure S3C), survival condition as compared with other clinical risk factors including age (>60 vs. ≤60), gender (male vs. female), smoking (smoker vs. nonsmoker), pathological stages (stage II vs. stage I), and *EGFR/ALK/KRAS* mutation status (mutation vs. wild-type) in patients with stages I/II LUAD. Moreover, the AIM2 mRNA levels in LUAD derived from male, smoker, wild-type *EGFR/ALK/KRAS* tumors, pathologic stage II tumors, and patients with cancer relapse were significantly higher than those derived from female, nonsmoker, *EGFR/ALK/KRAS*-mutated tumors, stage I tumors, and patients without cancer relapse, respectively (Figure 2E). In comparison with other driver mutations, LUAD with *EGFR* mutation showed relatively low mRNA levels of AIM2 (Figure S3D). However, AIM2 mRNA levels were not significantly different in primary tumors derived from patients stratified by age (>60 vs. ≤60) (Figure 2E).

### 3.3 | AIM2 upregulation enhances the metastatic potentials of LUAD cells in vitro and in vivo

To uncover a possible mechanism by which AIM2 upregulation promotes the aggressive evolution of LUAD, we next performed a computational simulation using the Gene Set Enrichment

Analysis (GSEA) program. First, we generated an AIM2 gene signature by using the Spearman correlation test against the mRNA coexpression status of AIM2 with other somatic genes included in the GeneChip Human Genome U133 Plus 2.0 Array in GSE31210 LUAD derived from smoker patients harboring wild-type *EGFR/ALK/KRAS* and according to the record for patients with or without cancer recurrence. Then, we used Spearman coefficient  $\rho$  values as the AIM2 gene signatures to perform GSEA simulation against Hallmark gene sets (Figure 3A). GSEA results demonstrated that the AIM2 gene signature obtained from LUAD classified as smoker/wild-type *EGFR/ALK/KRAS*/cancer recurrence, but not the smoker/wild-type *EGFR/ALK/KRAS*/cancer non-recurrence, appear to be positively correlated with the gene set for epithelial-mesenchymal transition (EMT) with a statistical significance at  $p < 0.0001$  (Figure 3B,C). Moreover, the AIM2 mRNA levels were shown to be negatively associated with the expression of epithelial-type markers *TJP1*, *OCLN*, *MUC1*, and *CDH1* but positively correlated with the expression of mesenchymal-type markers *FN1*, *SNAI1*, *VIM*, and *CDH2* in the tested GSE31210 LUAD (Figure 3D).

Reverse-transcription PCR results showed that A549 and HCC827 cells express a higher AIM2 mRNA level relative to H1355 and PC9 cells (Figure 4A). The AIM2 mRNA levels appeared to be positively correlated with cellular migration abilities, as well as cell growth rate (Figure S4A,B), in the tested LUAD cell lines (Figure 4B,C). Whereas AIM2 knockdown by its two independent shRNA clones dramatically suppressed the endogenous AIM2 mRNA and protein expression (Figure 4D) and cellular migration abilities (Figure 4E,F) in A549 cells, the enforced expression of exogenous AIM2 DNA appeared to elevate the intracellular mRNA and protein levels of AIM2 (Figure 4G) and potentiate the cellular migration ability (Figure 4H,I) in PC9 cells. Robustly, AIM2 knockdown reduced the lung colony-forming ability of A549 cells in the xenotransplantation of IL2Rg null mice (Figure 4J). In addition, AIM2 knockdown predominantly mitigated the EMT progression as judged by an increased level of E-type marker *CDH1* and the decreased levels of M-type markers *CDH2*, *VIM*, and *FN1* in A549 cells (Figure 4K); conversely, AIM2 overexpression reversed these features in PC9 cells (Figure 4L).

### 3.4 | AIM2 upregulation potentiates the expression of PD-L1 in smoker patients with LUAD without driver mutations

Gene Set Enrichment Analysis results also showed that the gene set related to interferon gamma (IFN- $\gamma$ ) response is highly correlated

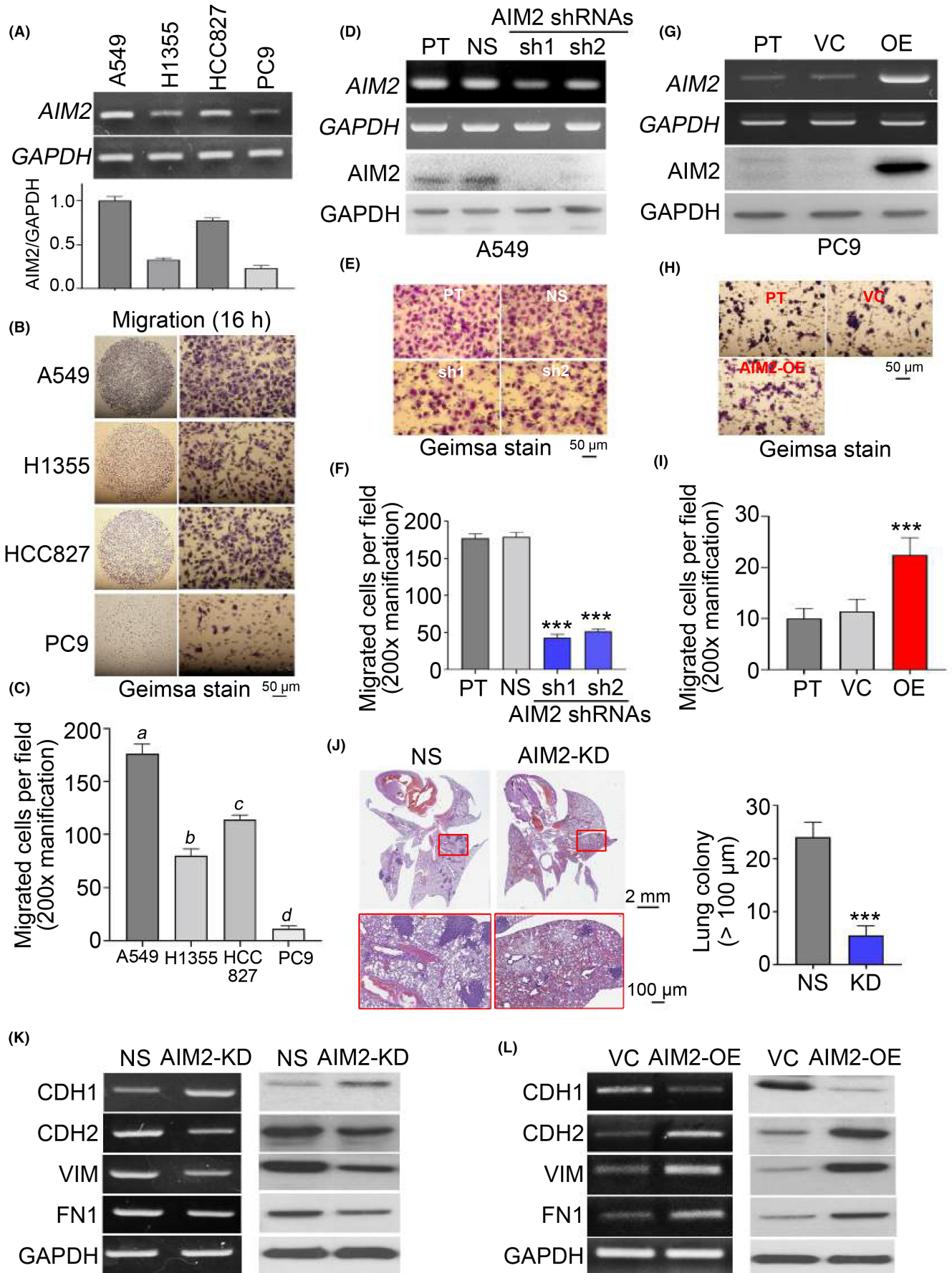


FIGURE 4 Legend on next page



**FIGURE 4** AIM2 knockdown suppresses the epithelial-mesenchymal transition (EMT) progression and metastatic potentials of lung adenocarcinoma cells. RT-PCR (upper) and Q-PCR (lower) for the endogenous mRNA levels of AIM2 and GAPDH (A); Giemsa stain for the migrated cells (B); and histogram for the migrated cell number, presented as mean  $\pm$  SEM, from three independent experiments of the 16-h transwell culture (C) against the tested lung adenocarcinoma cell lines A549, H1355, HCC827, and PC9. *p*-value, Friedman test. RT-PCR and immunoblotting for the mRNA and protein levels of AIM2 and GAPDH (D); Giemsa stain for the migrated cells (E); and histogram for the migrated cell number from three independent experiments of the 16-h transwell culture (F) against the parental (PT) A549 cells and A549 cells stably transfected with nonsilencing (NS) control or two independent AIM2 shRNAs. RT-PCR and immunoblotting for the mRNA and protein levels of AIM2 and GAPDH (G); Giemsa stain for the migrated cells (H); and histogram for the migrated cell number from three independent experiments of the 16-h transwell culture (I) against the parental (PT), vector control (VC), and AIM2-overexpressing (OE) PC9 cells. J, Hematoxylin/eosin stain for the appearance of tumors in lungs derived from the xenotransplantation of IL2Rg null mice ( $n = 5$ ) transplanted with the NS control or AIM2-KD A549 cells for 4 wk (upper) and histogram for the number of lung colonies that are larger than 100  $\mu$ m in diameter (lower). \*\*\* $p < 0.001$  (F, I, K) in the Mann-Whitney *U* test. K, L, RT-PCR (left) for the mRNA levels and Western blot analyses for the protein levels (right) of CDH1, CDH2, VIM, FN1, and GAPDH in the NS control/AIM2-knockdown (KD) A549 cells (K) and VC control/AIM2-OE PC9 cells (L). GAPDH was used as an internal control of experiments.

with AIM2 gene signatures derived from smoker patients with LUAD harboring wild-type *EGFR/ALK/KRAS* regardless of the status of cancer recurrence in the GSE31210 dataset (Figure 5A). Pearson correlation tests revealed that AIM2 expression causally associates with the mRNA levels of the IFN- $\gamma$  response gene set (Figure 5B) and PD-L1 (Figure 5C), which is an IFN- $\gamma$ -responsive gene. To validate these findings, we further dissected the coexpression of AIM2 with 200 genes included in the IFN- $\gamma$  response gene set and 47 genes related to immune checkpoint<sup>18</sup> in TCGA LUAD patients with smoking history and harboring wild-type *EGFR/ALK/KRAS* (Figure 5D). The data showed that AIM2 expression strongly ( $p < 0.0001$ ) correlates with the mRNA levels of IFN- $\gamma$  response and immune checkpoint gene sets (Figure 5E) and PD-L1 (Figure 5F). Interestingly, previous studies have demonstrated that IFN- $\gamma$  secreted from immune cells promotes tumor immune evasion via upregulating tumor immunosuppressive genes, for example, PD-L1,<sup>19</sup> and is capable of activating AIM2 inflammasome.<sup>20</sup> Therefore, these findings prompted us to delineate the role of AIM2 inflammasome in regulating the immunosuppression of LUAD.

AIM2 inflammasome activation has been shown to elevate the protein levels of secreted interleukin 1 $\beta$  (IL-1 $\beta$ ) and IL-18 and ultimately activate NF- $\kappa$ B.<sup>21</sup> Recent report has shown that AIM2 overexpression promotes but knockdown suppresses the activation of the inflammasome pathway as determined by the protein levels of ASC oligomerization, cleaved caspase-1, and cleaved/secreted IL-1 $\beta$  in NSCLC cells.<sup>22</sup> To confirm the activity of the inflammasome pathway, here we performed dot blot analyses and enzyme-linked immunosorbent assay (ELISA) to detect the protein levels of secreted IL-1 $\beta$  and IL-18, the products of inflammasome activation, in the AIM2-silenced A549 cells and AIM2-overexpressed PC9 cells. Dot blot analyses and ELISA indicated that AIM2 knockdown dramatically decreased but overexpression predominantly elevated the protein levels of secreted IL-1 $\beta$  and IL-18 in the cultivation of AIM2-silenced A549 cells and AIM2-overexpressed PC9 cells, respectively, as compared with control cells (Figure 6A). Either IL-1 $\beta$  or IL-18 neutralization effectively suppressed the migration ability of A549 cells, which partially mimics the outcome of AIM2 knockdown (Figure 55A,B). Accordingly, AIM2 knockdown predominantly suppressed but overexpression obviously promoted

NF- $\kappa$ B activity as determined by a reduced level of its phosphorylated (Ser536) protein and decreased transcriptional regulation ability (Figure 6B) in A549 cells and PC9 cells, respectively. In comparison with the control cells, the phosphorylated (Tyr701) protein level and transcriptional regulation ability of STAT1 were dramatically declined but markedly enhanced, respectively, in the AIM2-silenced A549 cells and AIM2-overexpressed PC9 cells (Figure 6C). Besides, AIM2 knockdown robustly repressed but overexpression dramatically elevated the endogenous mRNA level and cell surface expression of PD-L1 in the AIM2-silenced A549 cells and AIM2-overexpressed PC9 cells (Figure 6D), respectively. Moreover, the estimation for the association between AIM2 expression and immune infiltrates revealed that AIM2 expression is negatively correlated with LUAD purity but positively correlated with the infiltration level of IFN- $\gamma$ -producing CD8+ T cell, M1 macrophage, and NK cells in TCGA LUAD samples (Figure 6E). The inclusion of human recombinant IFN- $\gamma$  protein dose-dependently enhanced AIM2 expression in A549 cells (Figure 6F). These findings indicate the critical role of AIM2 inflammasome in the tumor immune microenvironment of LUAD.

Kaplan-Meier analyses demonstrated that the combination of higher PD-L1 and AIM2 expression refers to the poorest outcome in LUAD patients from the GSE31210 dataset and K-M Plotter database under the recurrence and first progression-free survival conditions (Figure 7A). Moreover, the treatment with NF- $\kappa$ B inhibitor BAY 11-7082 was found to predominantly reverse the expression of EMT markers CDH1 and CDH2 and repress PD-L1 expression in AIM2-overexpressing PC9 cells (Figure 7B).

## 4 | DISCUSSION

Driver mutations of genes, for example, *EGFR*, *ALK*, *KRAS*, etc., provide a therapeutic strategy to combat LUAD via targeting the enzymatic activity of these protein kinases. However, LUAD patients without these driver mutations are usually treated with tumor resection at the early pathologic stage or chemotherapy at the advanced stage. As a result, immunotherapies, such as immune-checkpoint inhibitors and anti-PD-1/PD-L1 agents, were

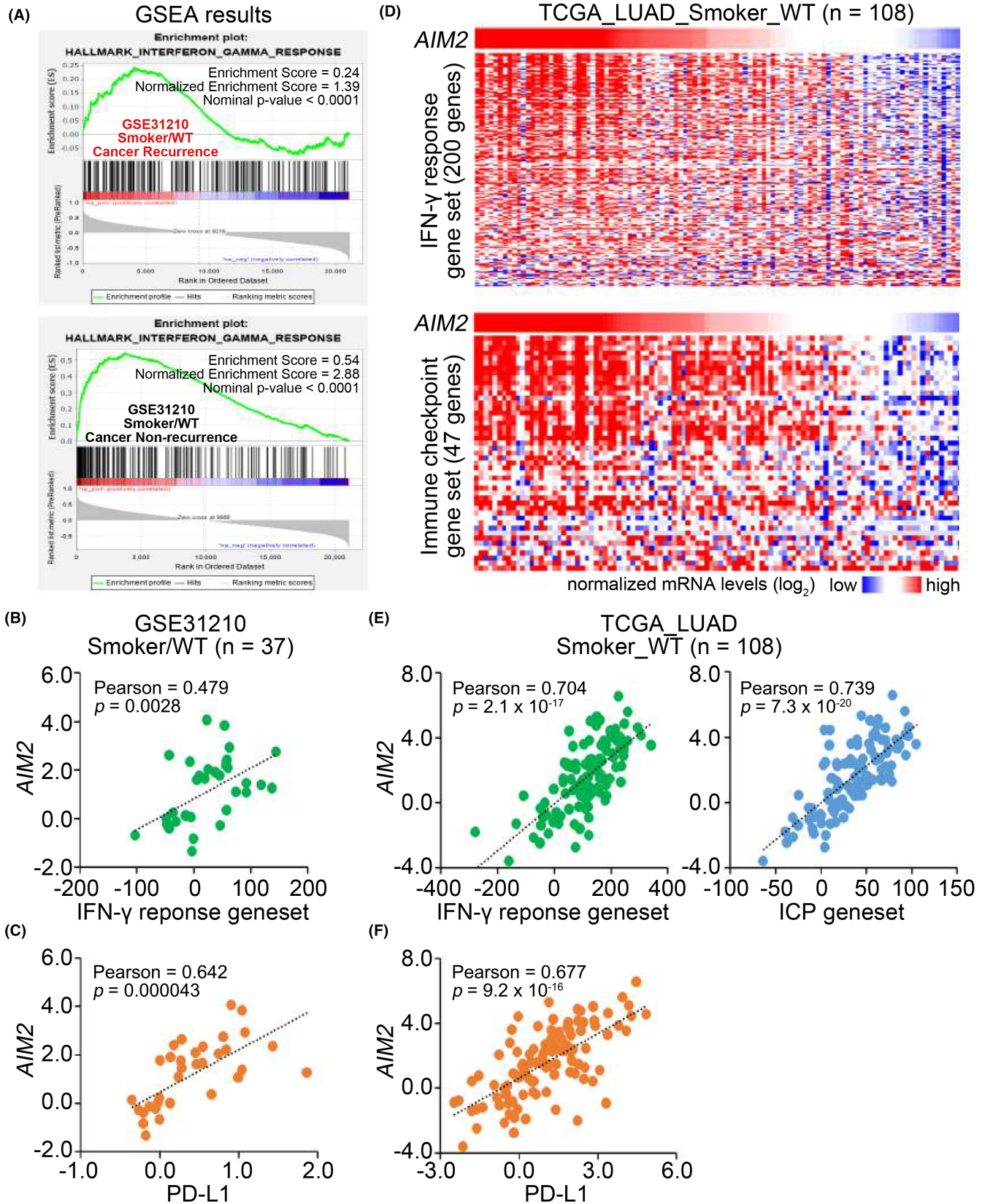


**FIGURE 5** AIM2 upregulation correlates with an increased level of immune checkpoint genes in lung adenocarcinoma (LUAD). A, The plot of enrichment scores for the correlation of AIM2-related gene signatures with the gene set for interferon gamma (IFN- $\gamma$ ) response in the indicated GSE31210 LUAD samples. B, C, Scatter plots for the mRNA levels of AIM2 versus IFN- $\gamma$  response gene set (B) and AIM2 versus PD-L1 (C) in the GSE31210 LUAD samples. D, E, Heatmap (D) and Scatter plots (E) for the transcriptional profiling of AIM2 versus IFN- $\gamma$  response gene set immune checkpoint (ICP) gene set using TCGA LUAD samples derived from patients recorded as smoker and harboring wild-type (WT) *EGFR/KRAS/ALK*. F, Scatter plot for the mRNA levels of AIM2 versus PD-L1 in TCGA LUAD samples shown in (D) and (E). P-values (B, C, E, F), Pearson correlation test.

currently proposed to treat LUAD without driver mutations. Thus, identifying a useful biomarker to predict the effectiveness of immunotherapies is urgently needed. Here we find that silencing AIM2 expression predominantly suppresses metastatic potentials

and PD-L1 expression probably via decreasing the transcriptional regulation ability of NF- $\kappa$ B and STAT1 in LUAD cells. Previous report showed that PD-L1 expression is regulated by NF- $\kappa$ B during EMT signaling in NSCLC.<sup>23</sup> On the other hand, the positive

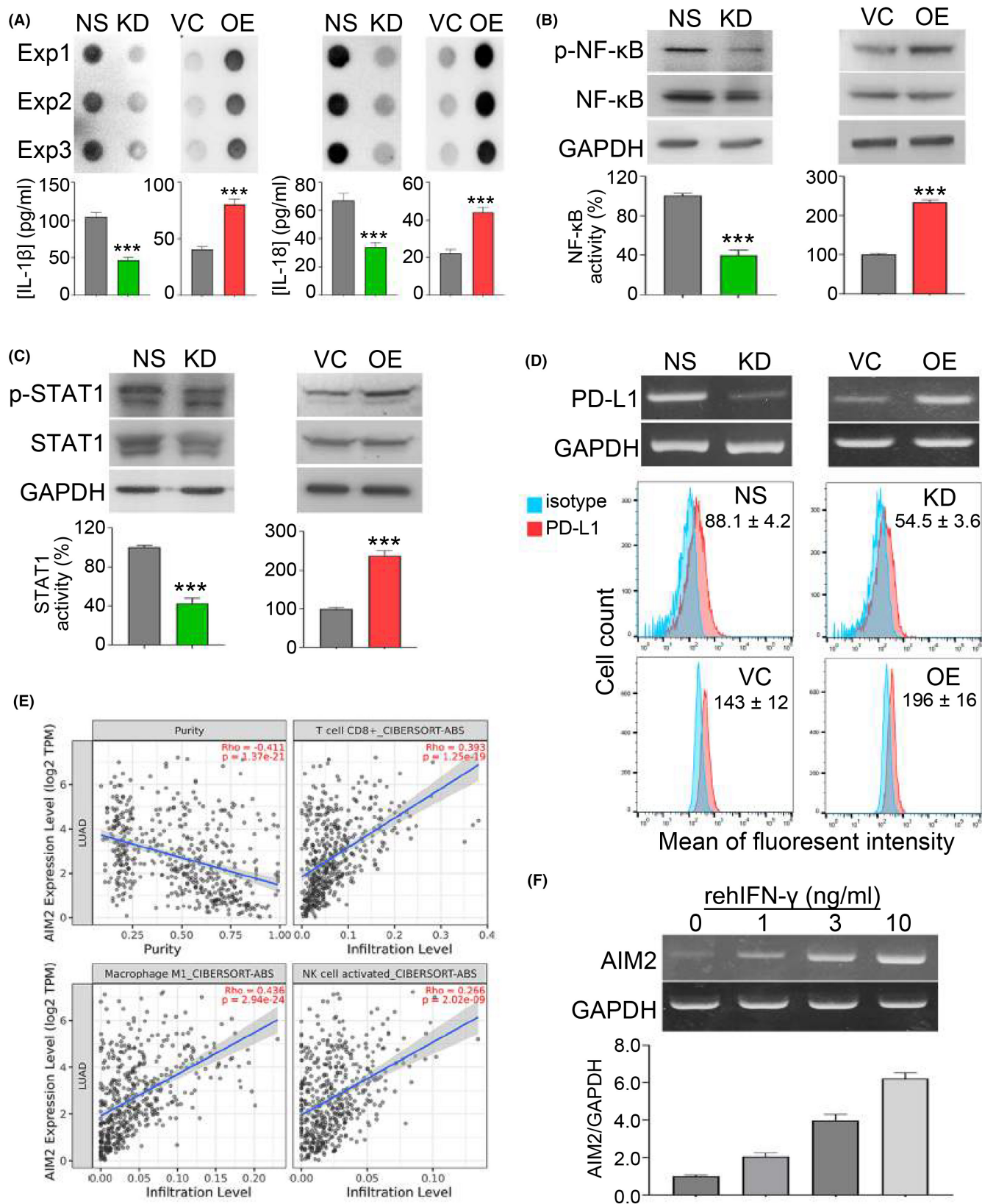
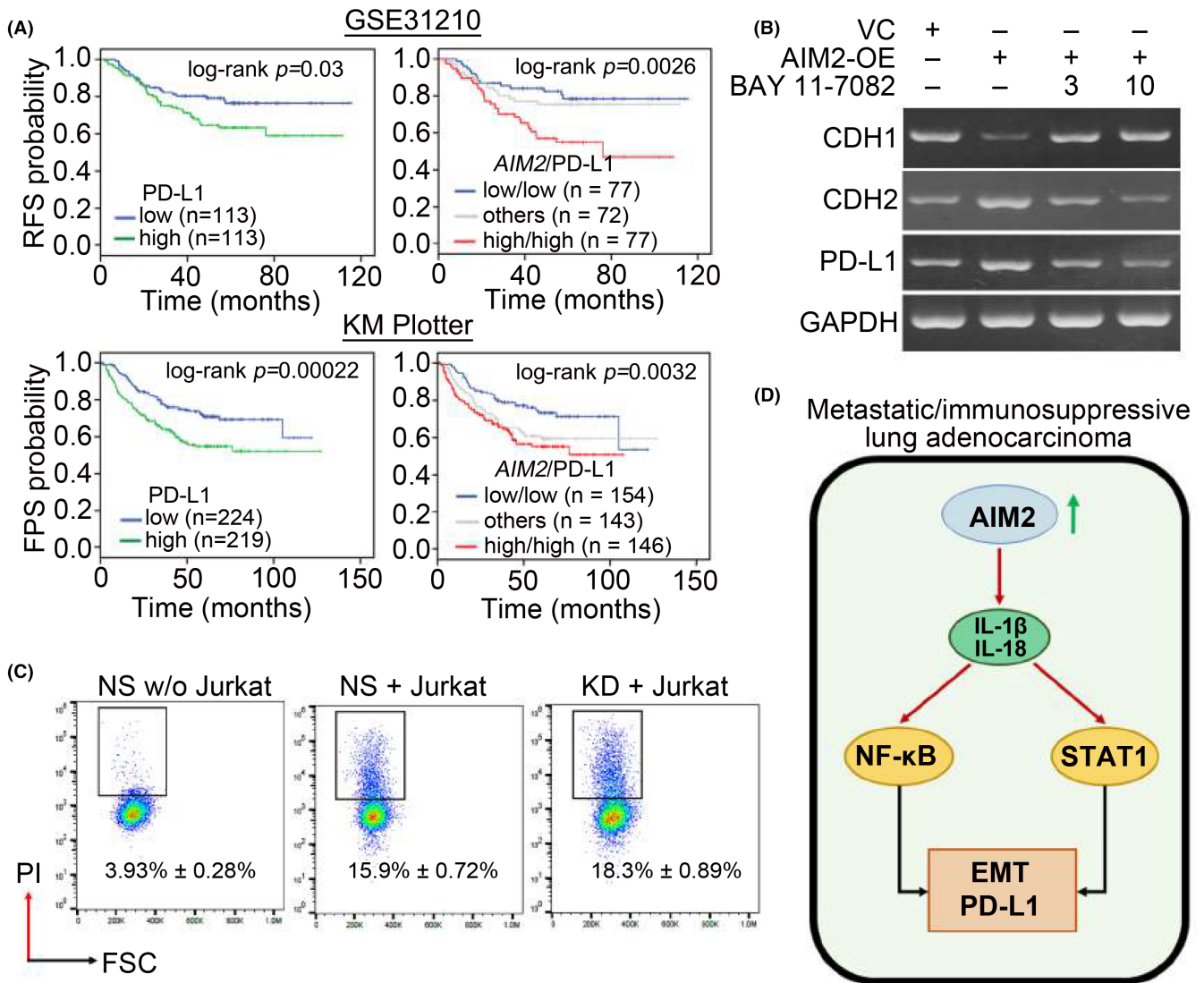


FIGURE 6 Legend on next page

**FIGURE 6** AIM2 knockdown suppresses the inflammasome-related signaling axis and IFN- $\gamma$  responsive pathway in lung adenocarcinoma (LUAD) cells. A, Dot blot analysis (upper) and ELISA (lower) for the protein levels of secreted IL-1 $\beta$  and IL-18 in the culture media from the three independent cultivation of NS control/AIM2-KD A549 cells and VC control/AIM2-OE PC9 cells. B, C, Western blot analysis for the protein levels of phosphorylated NF- $\kappa$ B (p-NF- $\kappa$ B), NF- $\kappa$ B, p-STAT1, STAT1, and GAPDH in the whole-cell lysates (B, C, upper) and Luciferase-reporter assay for the transcriptional regulator activity of NF- $\kappa$ B and STAT1 (B, C, lower) from the indicated A549 and PC9 cell variants. In (A-C), data from three independent experiments were presented as mean  $\pm$  SEM. \*\*\* $p < 0.001$  in the Mann-Whitney  $U$  test. D, RT-PCR for the mRNA levels of PD-L1 and GAPDH and flow-cytometric analyses for cell surface levels of PD-L1 in the indicated A549 and PC9 cell variants. E, The correlation among AIM2 mRNA levels, tumor purity, and infiltration levels of CD8+ T cells, M1 macrophage, and NK cells in TCGA LUAD samples. Spearman correlation test was used to estimate the statistical significance. F, RT-PCR (upper) and Q-PCR (lower) analyses for the mRNA levels of AIM2 and GAPDH in A549 cells treated with recombinant human IFN- $\gamma$  (rhIFN- $\gamma$ , Sino Biological) at indicated concentrations for 24h.



**FIGURE 7** Targeting AIM2 inflammasome pathway mitigates the PD-L1-mediated immunosuppression in lung adenocarcinoma (LUAD). A, Kaplan-Meier analyses under recurrence-free survival (RFS) for GSE31210 LUAD cohort (upper) and first progression-free survival (FPS) for K-M Plotter cohort (lower) conditions against the PD-L1 mRNA levels combined without (left) or with (right) AIM2 mRNA levels. B, RT-PCR for the mRNA levels of CDH1, CDH2, PD-L1, and GAPDH in the vector control (VC) and AIM2-overexpressing (OE) PC9 cells treated without or with NF- $\kappa$ B inhibitor BAY 11-7082 at 3 and 10  $\mu$ M. C, Flow cytometry analysis for the cell death of NS control A549 cells without (w/o) coculture with the activated Jurkat T cells and Jurkat T cell cytotoxicity against the NS control and AIM2-KD A549 cells. The proportions of apoptotic cells (CFSE+/PI+) from three independent experiments were presented as mean  $\pm$  SEM. D, The illustration of a possible mechanism for the AIM2-fostered epithelial-mesenchymal transition (EMT) progression and PD-L1 expression in metastatic/ immunosuppressive LUAD.

feedback regulation between PKD3 and PD-L1 could drive EMT of oral squamous cell carcinoma cells via activating the STAT1 pathway, thereby promoting tumor growth and metastasis.<sup>24</sup> In colorectal cancer, it has been found that PD-L1 expression is regulated by the IFN- $\gamma$ /JAK/STAT signaling pathway.<sup>25</sup> We thus proposed that the upregulation/activation of AIM2 inflammasome may foster the activation of NF- $\kappa$ B and STAT1 via elevating the extracellular IL-1 $\beta$  and IL-18 levels, which have been shown to reinforce the activity of NF- $\kappa$ B and STAT1 previously,<sup>26,27</sup> thereby promoting EMT progression and enhancing PD-L1 expression in the metastatic/immunosuppressive LUAD (Figure 7D).

Long-term smoking has been considered a risk factor for lung cancer development. Accordingly, the chronic inflammation of the pulmonary system because of cigarette smoking has been thought to be associated with an immunosuppressive tumor microenvironment in LUAD.<sup>28</sup> In comparison with nonsmoker patients, an increased mutational burden was shown to enhance the sensitivity to immune checkpoint inhibitors in NSCLC patients with smoking history.<sup>29</sup> A higher mutational burden has been correlated with a favorable response in NSCLC patients who received anti-PD-1 therapy.<sup>30</sup> In this study, AIM2 upregulation is dominant for LUAD derived from smoker patients compared with nonsmoker patients. Moreover, AIM2 knockdown dramatically suppressed the secretion of IL-1 $\beta$  and IL-18 and the activity of NF- $\kappa$ B in LUAD cells. As the IL-1 $\beta$ /NF- $\kappa$ B signaling axis plays a pivotal role in chronic lung inflammation in cigarette smokers,<sup>31</sup> the targeting of AIM2-related inflammasome complex could be a useful strategy to downregulate the expression of PD-L1, thereby suppressing the immune evasion ability of LUAD derived from smoker patients. However, further experiments are still needed to prove this therapeutic strategy in LUAD cells without driver mutations from smoker patients because the employed LUAD cell lines in this study are KRAS-mutated (A549 and H1355), EGFR-mutated (H1355, HCC827, and PC9), and ALK-mutated (PC9) cell lines.

The intracellular inflammatory responses have been highly correlated with the metastatic progression in many types of cancer.<sup>32-39</sup> The activation of NLRP3 inflammasome has also been shown to promote cancer metastasis.<sup>11,13,15,16,40,41</sup> Nevertheless, AIM2 downregulation has been correlated with a poorer prognosis, probably due to an increased metastatic potential, in renal cell carcinoma<sup>42</sup> and hepatocellular carcinoma.<sup>43</sup> In contrast to these findings, here we show that AIM2 is upregulated in primary tumors compared with normal tissues derived from TCGA lung cancer patients and serves as a poor prognostic marker in LUAD patients. Moreover, the expression of AIM2 appeared to causally associate with the metastatic potentials and PD-L1 expression in LUAD cells. Besides, our data revealed that NLRP3 is significantly downregulated in primary tumors compared with normal tissues in TCGA lung cancer database even though NLRP3 inflammasome has been shown to play a vital role in regulating the proliferation and migration of A549 LUAD cells.<sup>16</sup> Therefore, further experiments are needed to explore the roles of AIM2-inflammasome in regulating the malignant evolution

in different types of cancer and uncover the mechanism underlying the activation of NLRPs and AIM2 in LUAD.

Although AIM2 has been considered a double-stranded DNA sensor in the innate immunity,<sup>44</sup> the recent study demonstrated that the formation of the IL-1 $\beta$ /AIM2 feedback loop might play a critical role in promoting the metastatic progression in NSCLC.<sup>22</sup> Here, we show that IL-1 $\beta$  neutralization significantly reduces the cellular migration ability of A549 cells, which may implicate the existence of this feedback loop. Besides, it has been illustrated that guanylate-binding proteins (GBPs) may act as an upstream regulator in directing inflammasome subtype-specific responses and GBP2/5 is capable of triggering the activation of AIM2 inflammasome and the maturation of IL-1 $\beta$  and IL18.<sup>45</sup> Previously, we have reported that GBP5 upregulation promotes the metastatic potential and PD-L1 expression in triple-negative breast cancer.<sup>17</sup> Because GTP concentration is increased in the highly proliferative cancer cells via the Warburg effect,<sup>46</sup> we speculate that the increased GTP-binding activity of GBP5 in A549 cells with a rapid growth rate might be one of the factors for the activation of the AIM2 inflammasome pathway.

In conclusion, this study presents AIM2 as a poor prognostic biomarker and indicator for an elevated PD-L1 expression in LUAD. Moreover, therapeutic targeting of AIM2 expression and activity might be a useful strategy to suppress the metastatic progression and enhance immune surveillance against LUAD without driver mutations.

#### AUTHOR CONTRIBUTIONS

Study conception and design: J.-Q.Z., H.-W.C. and Y.-F.L. Development of methodology: J.-Q.Z., C.-H.L., H.-H.L., W.-M.C., L.-J.L., C.-Y.S., K.-Y.L., H.-W.C. and Y.-F.L. Analysis and interpretation of data: J.-Q.Z., C.-H.L. and H.-H.L. Writing, reviewing, and/or revision of the manuscript: J.-Q.Z., H.-W.C. and Y.-F.L.

#### ACKNOWLEDGEMENTS

The authors would like to thank the National RNAi Core Facility at Academia Sinica in Taiwan for providing shRNA reagents and related services.

#### FUNDING INFORMATION

This study was supported by the Ministry of Science and Technology, Taiwan (MOST 108-2314-B-038-016 and MOST 108-2320-B-038-017-MY3).

#### DISCLOSURE

The authors have no conflict of interest.

#### ETHICS STATEMENT

Approval of the research protocol by an Institutional Reviewer Board: N/A.

Informed Consent: N/A.

Registry and the Registration No. of the study/trial: N/A.

Animal Studies: All procedures of animal experiments were approved (LAC-2019-0060) by the Institutional Animal Care and Use Committee at Taipei Medical University.

## ORCID

Wei-Ming Chang  <https://orcid.org/0000-0002-6899-4043>

Hui-Wen Chiu  <https://orcid.org/0000-0002-5027-390X>

Yuan-Feng Lin  <https://orcid.org/0000-0003-4456-0766>

## REFERENCES

- Araujo A, Ribeiro R, Azevedo I, et al. Genetic polymorphisms of the epidermal growth factor and related receptor in non-small cell lung cancer – a review of the literature. *Oncologist*. 2007;12:201-210.
- Wu K, House L, Liu W, Cho WCS. Personalized targeted therapy for lung cancer. *Int J Mol Sci*. 2012;13:11471-11496.
- Tamura T, Kurishima K, Nakazawa K, et al. Specific organ metastases and survival in metastatic non-small-cell lung cancer. *Mol Clin Oncol*. 2015;3:217-221.
- Mantovani A, Allavena P, Sica A, Balkwill F. Cancer-related inflammation. *Nature*. 2008;454:436-444.
- Bremnes RM, Al-Shibli K, Donnem T, et al. The role of tumor-infiltrating immune cells and chronic inflammation at the tumor site on cancer development, progression, and prognosis: emphasis on non-small cell lung cancer. *J Thorac Oncol*. 2011;6:824-833.
- Awad F, Assrawi E, Jumeau C, et al. Impact of human monocyte and macrophage polarization on NLR expression and NLRP3 inflammasome activation. *PLoS One*. 2017;12:e0175336.
- Yu CH, Moecking J, Geyer M, Masters SL. Mechanisms of NLRP1-mediated autoinflammatory disease in humans and mice. *J Mol Biol*. 2018;430:142-152.
- Allen IC, TeKippe EM, Woodford RM, et al. The NLRP3 inflammasome functions as a negative regulator of tumorigenesis during colitis-associated cancer. *J Exp Med*. 2010;207:1045-1056.
- Raut PK, Kim SH, Choi DY, Jeong GS, Park PH. Growth of breast cancer cells by leptin is mediated via activation of the inflammasome: critical roles of estrogen receptor signaling and reactive oxygen species production. *Biochem Pharmacol*. 2019;161:73-88.
- Jin H, Ko YS, Kim HJ. P2Y2R-mediated inflammasome activation is involved in tumor progression in breast cancer cells and in radiotherapy-resistant breast cancer. *Int J Oncol*. 2018;53:1953-1966.
- Hu Q, Zhao F, Guo F, Wang C, Fu Z. Polymeric nanoparticles induce NLRP3 inflammasome activation and promote breast cancer metastasis. *Macromol Biosci*. 2017;17:1700273.
- Bae JY, Lee SW, Shin YH, Lee JH, Jahng JW, Park K. P2X7 receptor and NLRP3 inflammasome activation in head and neck cancer. *Oncotarget*. 2017;8:48972-48982.
- Wang H, Wang Y, Du Q, et al. Inflammasome-independent NLRP3 is required for epithelial-mesenchymal transition in colon cancer cells. *Exp Cell Res*. 2016;342:184-192.
- Xu Y, Li H, Chen W, et al. Mycoplasma hyorhinis activates the NLRP3 inflammasome and promotes migration and invasion of gastric cancer cells. *PLoS One*. 2013;8:e77955.
- Zou J, Yang Y, Yang Y, Liu X. Polydatin suppresses proliferation and metastasis of non-small cell lung cancer cells by inhibiting NLRP3 inflammasome activation via NF-kappaB pathway. *Biomed Pharmacother*. 2018;108:130-136.
- Wang Y, Kong H, Zeng X, et al. Activation of NLRP3 inflammasome enhances the proliferation and migration of A549 lung cancer cells. *Oncol Rep*. 2016;35:2053-2064.
- Cheng SW, Chen PC, Lin MH, et al. GBP5 repression suppresses the metastatic potential and PD-L1 expression in triple-negative breast cancer. *Biomedicine*. 2021;9:371.
- De SM, Arrigoni A, Rossetti G, et al. Transcriptional landscape of human tissue lymphocytes unveils uniqueness of tumor-infiltrating T regulatory cells. *Immunity*. 2016;45:1135-1147.
- Mojic M, Takeda K, Hayakawa Y. The dark side of IFN-gamma: its role in promoting cancer immunoevasion. *Int J Mol Sci*. 2017;19:89.
- Wallet P, Benaoudia S, Mosnier A, et al. IFN-gamma extends the immune functions of guanylate binding proteins to inflammasome-independent antibacterial activities during *Francisella novicida* infection. *PLoS Pathog*. 2017;13:e1006630.
- Schroder K, Tschopp J. The inflammasomes. *Cell*. 2010;140:821-832.
- Zhang M, Jin C, Yang Y, et al. AIM2 promotes non-small-cell lung cancer cell growth through inflammasome-dependent pathway. *J Cell Physiol*. 2019;234:20161-20173.
- Asgarova A, Asgarov K, Godet Y, et al. PD-L1 expression is regulated by both DNA methylation and NF-kB during EMT signaling in non-small cell lung carcinoma. *Onco Targets Ther*. 2018;7:e1423170.
- Cui B, Chen J, Luo M, et al. PKD3 promotes metastasis and growth of oral squamous cell carcinoma through positive feedback regulation with PD-L1 and activation of ERK-STAT1/3-EMT signalling. *Int J Oral Sci*. 2021;13:8.
- Zhao T, Li Y, Zhang J, Zhang B. PD-L1 expression increased by IFN-gamma via JAK2-STAT1 signaling and predicts a poor survival in colorectal cancer. *Oncol Lett*. 2020;20:1127-1134.
- Lee KM, Kang JH, Yun M, Lee SB. Quercetin inhibits the poly(dA:dT)-induced secretion of IL-18 via down-regulation of the expressions of AIM2 and pro-caspase-1 by inhibiting the JAK2/STAT1 pathway in IFN-gamma-primed human keratinocytes. *Biochem Biophys Res Commun*. 2018;503:116-122.
- Pugazhenth S, Zhang Y, Bouchard R, Mahaffey G. Induction of an inflammatory loop by interleukin-1beta and tumor necrosis factor-alpha involves NF-kB and STAT-1 in differentiated human neuroprogenitor cells. *PLoS One*. 2013;8:e69585.
- Sato K, Mimaki S, Yamashita R, et al. Association between the mutational smoking signature and the immune microenvironment in lung adenocarcinoma. *Lung Cancer*. 2020;147:12-20.
- Sun LY, Cen WJ, Tang WT, et al. Smoking status combined with tumor mutational burden as a prognosis predictor for combination immune checkpoint inhibitor therapy in non-small cell lung cancer. *Cancer Med*. 2021;10:6610-6617.
- Li B, Huang X, Fu L. Impact of smoking on efficacy of PD-1/PD-L1 inhibitors in non-small cell lung cancer patients: a meta-analysis. *Onco Targets Ther*. 2018;11:3691-3696.
- Yi G, Liang M, Li M, et al. A large lung gene expression study identifying IL1B as a novel player in airway inflammation in COPD airway epithelial cells. *Inflamm Res*. 2018;67:539-551.
- Hibino S, Kawazoe T, Kasahara H, et al. Inflammation-induced tumorigenesis and metastasis. *Int J Mol Sci*. 2021;22:5421.
- Liu Z, Ding F, Shen X. Total flavonoids of *Radix Tetrastigma* suppress inflammation-related hepatocellular carcinoma cell metastasis. *Mol Genet Genomics*. 2021;296:571-579.
- Tang YM, Cao QY, Guo XY, et al. Inhibition of p38 and ERK1/2 pathways by sparstolonin B suppresses inflammation-induced melanoma metastasis. *Biomed Pharmacother*. 2018;98:382-389.
- Archer M, Dogra N, Kyprianou N. Inflammation as a driver of prostate cancer metastasis and therapeutic resistance. *Cancers (Basel)*. 2020;12:2984.
- Ershaid N, Sharon Y, Doron H, et al. NLRP3 inflammasome in fibroblasts links tissue damage with inflammation in breast cancer progression and metastasis. *Nat Commun*. 2019;10:4375.
- Gobel A, Dell'Endice S, Jaschke N, et al. The role of inflammation in breast and prostate cancer metastasis to bone. *Int J Mol Sci*. 2021;22:5078.
- Wang H, Yao L, Gong Y, Zhang B. TRIM31 regulates chronic inflammation via NF-kappaB signal pathway to promote invasion and metastasis in colorectal cancer. *Am J Transl Res*. 2018;10:1247-1259.

39. Wellenstein MD, Coffelt SB, Duits DEM, et al. Loss of p53 triggers WNT-dependent systemic inflammation to drive breast cancer metastasis. *Nature*. 2019;572:538-542.
40. Fan SH, Wang YY, Lu J, et al. Luteoloside suppresses proliferation and metastasis of hepatocellular carcinoma cells by inhibition of NLRP3 inflammasome. *PLoS One*. 2014;9:e89961.
41. Wang K, Xu T, Ruan H, et al. LXRalpha promotes cell metastasis by regulating the NLRP3 inflammasome in renal cell carcinoma. *Cell Death Dis*. 2019;10:159.
42. Chai D, Shan H, Wang G, et al. AIM2 is a potential therapeutic target in human renal carcinoma and suppresses its invasion and metastasis via enhancing autophagy induction. *Exp Cell Res*. 2018;370:561-570.
43. Chen SL, Liu LL, Lu SX, et al. HBx-mediated decrease of AIM2 contributes to hepatocellular carcinoma metastasis. *Mol Oncol*. 2017;11:1225-1240.
44. Hornung V, Ablasser A, Charrel-Dennis M, et al. AIM2 recognizes cytosolic dsDNA and forms a caspase-1-activating inflammasome with ASC. *Nature*. 2009;458:514-518.
45. Kim BH, Chee JD, Bradfield CJ, Park ES, Kumar P, MacMicking JD. Interferon-induced guanylate-binding proteins in inflammasome activation and host defense. *Nat Immunol*. 2016;17:481-489.
46. Cassim S, Raymond VA, Dehbidi-Assadzadeh L, Lapierre P, Bilodeau M. Metabolic reprogramming enables hepatocarcinoma cells to efficiently adapt and survive to a nutrient-restricted microenvironment. *Cell Cycle*. 2018;17:903-916.

#### SUPPORTING INFORMATION

Additional supporting information can be found online in the Supporting Information section at the end of this article.

**How to cite this article:** Zheng J-Q, Lin C-H, Lee H-H, et al. AIM2 upregulation promotes metastatic progression and PD-L1 expression in lung adenocarcinoma. *Cancer Sci*. 2023;114:306-320. doi: [10.1111/cas.15584](https://doi.org/10.1111/cas.15584)